Eur. Phys. J. D **2**, 83–87 (1998)

THE EUROPEAN PHYSICAL JOURNAL D

A matrix study of the transfer of polarized radiation in plasmas. Application to neon-like germanium lasers

D. Benredjem[1,a], V. Bommier[2], H. Guennou[1], C. Möller[1], and A. Sureau[1]

[1] Laboratoire de Spectroscopie Atomique et Ionique[b], Université Paris-Sud, Bâtiment 350, 91405 Orsay Cedex, France
[2] Laboratoire Atomes et Molécules en Astrophysique[c], Observatoire de Paris, Section de Meudon, 92195 Meudon, France

Received: 10 October 1997 / Revised: 12 January 1998 / Accepted: 27 January 1998

Abstract. In order to solve the radiative-transfer equation for polarized beams propagating in plasmas a matrix approach is applied. The solution is the four-components Stokes vector, and the effect of the medium on the state of the radiation is represented by an amplification operator. Our approach is applied to the neon-like germanium 23.6 nm line, when a right-circularly polarized beam is injected into an amplifying plasma. The conditions governing the recovery of the initial polarization state are investigated over the entire spectrum of the output.

PACS. 42.55.Vc X- and γ-ray lasers – 42.68.Ay Propagation, transmission, attenuation, and radiative transfer – 32.80.-t Photon interactions with atoms

Since the demonstration of amplification in Ne-like Se [1] the development of high-brightness X-ray lasers (XRL) has been at the centre of a worldwide effort, and lasing in several other systems has been achieved [2]. Amplification around 20 nm has been reported by several groups [3–5]. The Ni-like isoelectronic sequence presents a promising way towards the water window. Using the RAL laser facility, Zhang and co-workers have obtained a saturated emission at 14 nm in Ag [6]. Attention has recently turned to the investigation of output properties such as spatial coherence [7,8] and polarization [9,10] in order to produce sources suitable for biological-microscopy [11], holography [12], and interferometry [13,14] applications.

In a previous work [15] we investigated the influence of a plasma on the polarization state of X-UV radiation. In this paper the polarization evolution is studied by developing a general formalism where the solution is the four-components Stokes vector, and where the absorption and induced-emission processes are represented by a 4×4 matrix. We consider a radiation which results from (*i*) the $J'M' \rightarrow JM$ transitions between two levels (fixed J' and J), and (*ii*) a possible -totally polarized- incident beam whose frequency corresponds to the above transitions, and whose effect consists in generating population differences among the states of each level, thus polarizing the medium. Owing to the XRL irradiance conditions, the resulting plasma is generally well represented by a cylindrical column whose axis is taken to be the z axis of a right-handed coordinate system xyz. As the XRL beam propagates parallel to this axis, only circularly polarized waves (σ_+ and σ_-) can be amplified. Using the Bloch relation for the density matrix, and the Maxwell wave equation for the electric-field propagation, one obtains the rate equations governing the evolution of the quantum-state populations n_{JM} [16].

An incident σ_+ beam, which is the output of a first plasma referred to as the injector, is seeded in a second plasma (the amplifier). The intensity $I_{\rm inc}$ of the incident beam is given by $I_{\rm inc} = S[\exp(Gl_{\rm inj}) - 1]$, where S is the source function, G the local gain, and $l_{\rm inj}$ the injector length. Figure 1 shows the amplifier quantum-state populations n_{1M} and n_{2M} involved in the Ge^{22+} $2-1$ lasing line (23.6 nm). In the absence of a polarized incident beam, the populations are equal for M and $-M$ states. The atomic orientation is thus zero, which means that the medium cannot generate a circularly polarized output, *i.e.*, there is no spontaneous polarization. When a σ_+ wave of intensity $I_{\rm inc} = 2.7 \times 10^5$ W/cm^2 ($S = 25.2$ W/cm^2, $G = 9.28$ cm^{-1}, and $l_{\rm inj} = 1$ cm), is injected in the amplifier, the n_{1M}'s are enhanced while the n_{2M}'s are reduced by a larger amount, compared to the populations calculated in the absence of incident beam. Concerning $J = 2$, the depletion is stronger for higher M (*cf.* relative line strengths), as long as the intensity of the σ_- wave remains below saturation. At large propagation lengths saturation is achieved for σ_+, and σ_- begins to saturate, yielding smaller and smaller $|n_{2M} - n_{2-M}|$ differences. Under the

[a] e-mail: djamel.benredjem@lsai.u-psud.fr
[b] URA 775 du CNRS
[c] URA 812 du CNRS

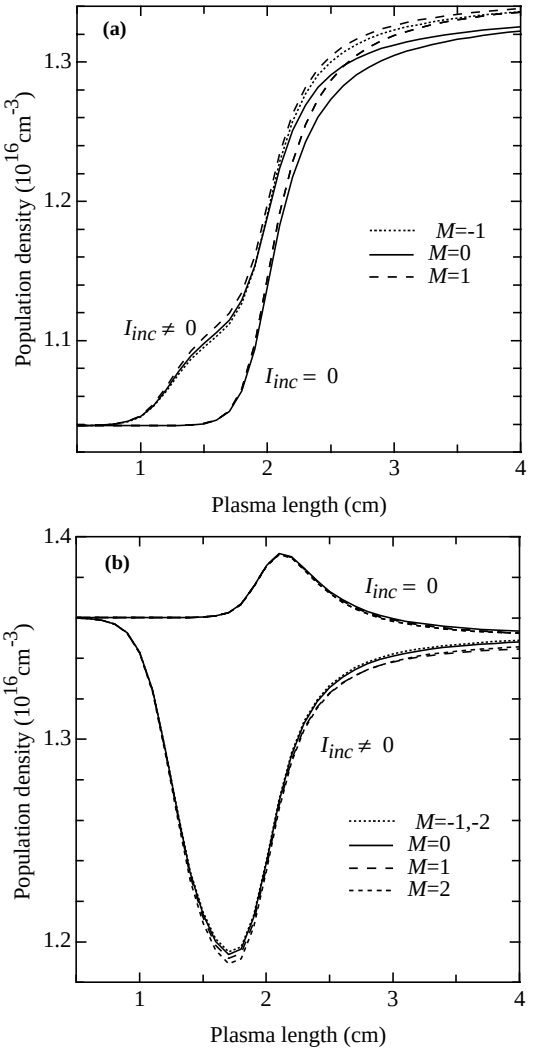

Fig. 1. Population density of the states involved in the Ge^{22+} 2−1 lasing line (23.6 nm), namely $|(2p^5 3s)1M>$ (a) and $|(2p^5 3p)2M>$ (b), as a function of amplifier length. $I_{\rm inc} \neq 0$ indicates the presence of an incident σ_+ radiation which is the output of 1 cm long injector. The electron density is equal to 7×10^{20} cm^{-3}, and the electron and ion temperatures are $T_{\rm e} = 500$ eV and $T_{\rm i} = 300$ eV. These values are representative of saturated lasers.

dominant σ_+ field, to the most depleted $|2M\rangle$ states correspond the most fed $|1M-1\rangle$ states. As a result, $|11\rangle$ is more populated than $|1-1\rangle$. Owing to the elastic electron-ion collisions $|JM\rangle + {\rm e}^- \rightarrow |JM'\rangle + {\rm e}^-(M' \neq M)$, whose rate is large enough to equally re-distribute the ions among the quantum states of each laser level, the orientation and alignment are very small.

The resolution of the radiative-transfer equation (RTE) consists in finding the four Stokes parameters $I^{(p)}(p = 0{-}3)$, where $I^{(0)}$ denotes total intensity, while $I^{(1)}$ and $I^{(2)}$ involve linear polarization, and $I^{(3)}$ circular polarization. For a beam propagating with frequency ν, in a small solid angle Ω centered on the z axis, the inhomogeneous RTE is

$$\frac{\partial \mathbf{I}(z,\nu,\Omega)}{\partial z} = -\overline{\mathbf{K}}(z,\nu,\Omega)\mathbf{I}(z,\nu,\Omega) + \mathbf{J}(z,\nu,\Omega), \quad (1)$$

where $\overline{\mathbf{K}}$ is the 4×4 matrix which describes the absorption, induced-emission, and anomalous-dispersion processes. This matrix is written

$$\overline{\mathbf{K}} = -\begin{pmatrix} G^{(0)} & G^{(1)} & G^{(2)} & G^{(3)} \\ G^{(1)} & G^{(0)} & -[U^{(3)} - W^{(3)}] & U^{(2)} - W^{(2)} \\ G^{(2)} & U^{(3)} - W^{(3)} & G^{(0)} & -[U^{(1)} - W^{(1)}] \\ G^{(3)} & -[U^{(2)} - W^{(2)}] & U^{(1)} - W^{(1)} & G^{(0)} \end{pmatrix} \quad (2)$$

Assuming that the Zeeman coherences $\langle JM|\rho|JM'\rangle$ (non-diagonal elements of the density matrix in each J level) are zero, the absorption properties of the medium, with respect to the different polarization states of the radiation field, are represented by the components

$$K^{(p)}(z,\nu,\Omega) = \frac{3}{4\pi} B h\nu_0 (2J+1)\Phi(\nu) \times \sum_{M,N,q} n_{JN}(z) \begin{pmatrix} J' & J & 1 \\ -M & N & q \end{pmatrix}^2 \mathcal{T}^{(p)}_{-q,-q}(\Omega), \quad (3)$$

where B is the Einstein coefficient for absorption, Φ the normalized lineshape, and ν_0 the corresponding central frequency. Φ is calculated numerically using a very robust and reliable code [17] which accounts for electron-ion collisions and dynamic ion Stark broadening. The tensors $\mathcal{T}^{(p)}_{q,q'}$, defined in appendix 1 of reference [18], can be expressed in terms of the rotation matrices relative to the angles of the rotation bringing the polarization unit vectors $\mathbf{e}_{\pm 1}[\mathbf{e}_{\pm 1} = (\mp\mathbf{i} + i\mathbf{j})/\sqrt{2}]$ and $\mathbf{e}_0[\mathbf{e}_0 = \mathbf{k}]$ on the unit vectors $\mathbf{i}$, $\mathbf{j}$, $\mathbf{k}$ of the right-handed coordinate system xyz. The $p = 0$ component describes the absorption process, irrespective of the polarization state, while the $p = 1{-}3$ components account for the coupling, due to absorption, of $I^{(0)}$ with $I^{(1)}$, $I^{(2)}$, and $I^{(3)}$, respectively.

The $U^{(r)}(r = 1{-}3)$ components

$$U^{(r)} = K^{(r)}\{\Phi \rightarrow \Psi\}, \quad (4)$$

which involve absorption, describe the cyclical coupling of $I^{(1)}$, $I^{(2)}$, and $I^{(3)}$ with each other as a consequence of anomalous dispersion. $U^{(r)}$ is obtained from $K^{(r)}$ with the condition that Φ is replaced by the dispersion profile Ψ, responsible for the anomalous-dispersion effects which can play a significant role in many radiative-transfer situations. Ψ is the imaginary part of the complex profile $\Pi(\nu) = \Phi(\nu) + i\Psi(\nu)$. If Φ is taken to be a Voigt function (negligible Stark broadening) then Ψ is well represented by a Faraday-Voigt function. Even in the absence of magnetic field, the dispersion effects could be important in the saturation regime where the atomic polarization of the laser levels is generally finite. For an X-ray beam propagating

$$\bar{O}(z,z') = \exp[G^{(0)}(z-z')] \begin{pmatrix} \cosh[\Lambda_1(z-z')] & 0 & 0 & -S(G)\sinh[\Lambda_1(z-z')] \\ 0 & \cos[\Lambda_2(z-z')] & -S(U)\sin[\Lambda_2(z-z')] & 0 \\ 0 & S(U)\sin[\Lambda_2(z-z')] & \cos[\Lambda_2(z-z')] & 0 \\ -S(G)\sinh[\Lambda_1(z-z')] & 0 & 0 & \cosh[\Lambda_1(z-z')] \end{pmatrix} \tag{11}$$

along the z direction, Ψ is not involved in the final results. The total emission vector $\mathbf{J}$ (Eq. (1)) accounts for spontaneous emission. Its four components are given by

$$J^{(p)} = \alpha^{-1} K^{(p)}\{n_{JN} \to n_{J'M}\} \text{ with } \alpha = \frac{2J+1}{2J'+1}\frac{B}{A} \tag{5}$$

where A is the spontaneous-emission rate. The induced-emission components can be expressed in a rather compact form:

$$H^{(p)} = \alpha J^{(p)}. \tag{6}$$

Finally, the $W^{(r)}$'s, which play the same role for induced emission as the $U^{(r)}$'s for absorption, are

$$W^{(r)} = U^{(r)}\{n_{JN} \to n_{J'M}\}. \tag{7}$$

To obtain the absorption matrix corrected for induced emission (Eq. (2)) we have set $G^{(p)} = H^{(p)} - K^{(p)}$.

Taking into account the properties of the tensors $\mathcal{T}^{(p)}_{q,q'}$, for a beam propagating along the z axis, we can show that $K^{(1)}$, $K^{(2)}$, $H^{(1)}$, and $H^{(2)}$ are equal to zero, and one thus obtains a more tractable $\overline{\mathbf{K}}$ matrix

$$\overline{\mathbf{K}} = -\begin{pmatrix} G^{(0)} & 0 & 0 & G^{(3)} \\ 0 & G^{(0)} & -[U^{(3)} - \beta J^{(3)}] & 0 \\ 0 & U^{(3)} - \beta J^{(3)} & G^{(0)} & 0 \\ G^{(3)} & 0 & 0 & G^{(0)} \end{pmatrix}, \tag{8}$$

where $\beta[=\beta(\nu)] = \alpha\Psi(\nu)/\Phi(\nu)$.

The formal solution of the inhomogeneous RTE is given in terms of the amplification operator $\bar{O}$:

$$\mathbf{I}(z) = \int_{z0}^{z} \mathrm{d}z' \bar{O}(z,z')\mathbf{J}(z') + \bar{O}(z,z_0)\mathbf{I}(z_0), \tag{9}$$

where $z - z_0$ is the propagation length. The first contribution in the rhs accounts for emission in the interval $[z_0, z]$, while the second one is related to an incident beam penetrating into the amplifier with the Stokes vector $\mathbf{I}(z_0)$. In the framework of non-relativistic quantum electrodynamics, $\bar{O}$ may be written as [18]:

$$\begin{aligned} \bar{O}(z,z') = &\exp\left[G^{(0)}(z-z')\right] \\ &\times \left\{ \frac{1}{2}[\cosh[\Lambda_1(z-z')] + \cos[\Lambda_2(z-z')]]\overline{\mathbf{M}}_1 \right. \\ &- \sin[\Lambda_2(z-z')]\overline{\mathbf{M}}_2 - \sinh[\Lambda_1(z-z')]\overline{\mathbf{M}}_3 \\ &\left. + \frac{1}{2}\left[\cosh[\Lambda_1(z-z')] - \cos[\Lambda_2(z-z')]\right]\overline{\mathbf{M}}_4 \right\}. \end{aligned} \tag{10}$$

In the case of a beam propagating along the z axis with a small divergence, we have $\Lambda_1 = |G^{(3)}|$ and $\Lambda_2 = |U^{(3)} - \beta J^{(3)}|$. $\overline{\mathbf{M}}_1$ is the 4×4 identity matrix. After a straightforward calculation we can show that the sole non-zero matrix elements of the three other matrices $\overline{\mathbf{M}}_i$ are $\overline{\mathbf{M}}_2(2,3) = -\overline{\mathbf{M}}_2(3,2) = S(U)$, $\overline{\mathbf{M}}_3(1,4) = \overline{\mathbf{M}}_3(4,1) = S(G)$, $\overline{\mathbf{M}}_4(1,1) = \overline{\mathbf{M}}_4(4,4) = -\overline{\mathbf{M}}_4(2,2) = -\overline{\mathbf{M}}_4(3,3) = 1$, where $S(G) = -G^{(3)}/\Lambda_1$ and $S(U) = [U^{(3)} - \beta J^{(3)}]/\Lambda_2$. It is then easy to show that $\bar{O}$ takes the form:

see equation (11) *above.*

It is justified to partition the amplifier along the direction of propagation of the XRL beam in m intervals of small lengths $z_1 - z_{l-1} (l = 1, 2, ...m)$, with $z_m - z_0$ equal to the propagation length. Assuming the medium homogeneous in each segment, we can show that the solution of equation (1) is

$$\begin{aligned} \mathbf{I}(z) = &\bar{O}_m\bar{O}_{m-1}\ldots\bar{O}_2\bar{O}_1\mathbf{I}(z_0) + \mathbf{V}_m \\ &+ \sum_{l=1}^{m-1} \bar{O}_m\bar{O}_{m-1}\ldots\bar{O}_{l+1}\mathbf{V}_l, \end{aligned} \tag{12}$$

where each l-indexed quantity is constant in $[z_{l-1}, z_l]$.

The vectors $\mathbf{V}_l$ are given by

$$\mathbf{V}_l = \int_{z_{l-1}}^{z_l} \mathrm{d}z \left[\exp[-(z_l - z)\overline{\mathbf{K}}_l]\right]\mathbf{J}(z), \tag{13}$$

with $\mathbf{J}(z) = \left(J^{(0)}(z)\ 0\ 0\ J^{(3)}(z)\right)^{\dagger}$ ($\dagger$ means transpose). $\mathbf{V}_l$ is the Stokes vector corresponding to a wave emitted and amplified in the lth interval. The successive applications of $\bar{O}_{l+1}$, $\bar{O}_{l+2}$, ..., and $\bar{O}_m$ describe the amplification in the $(l+1)$th, $(l+2)$th, ... , and mth intervals, respectively. Without incident beam or with an unpolarized incident beam, $G^{(3)} = 0$ because $K^{(3)}$ and $J^{(3)}$ are themselves equal to zero, and the only non-zero component of $\mathbf{V}$ is thus $V^{(0)}$. It is then easy to show that $V_l^{(0)} = [J_l^{(0)}/G_l^{(0)}][\exp[G_l^{(0)}(z_l - z_{l-1})] - 1]$, which is the well-known solution of the RTE for unpolarized radiation, with $J_l^{(0)}$ designating the emissivity and $G_l^{(0)}$ the local gain. In our more general case, the $\mathbf{V}_l$'s are obtained through a straightforward calculation involving a Taylor expansion of the exponential in equation (13), followed by applications of $[\overline{\mathbf{K}}_l]^s (s = 0, 1, 2, ...)$ to $\mathbf{J}$, and finally by an integration. As $V_l^{(1)} = V_l^{(2)} = 0$, only the (1,1), (1,4), (4,1), and (4,4) elements of the matrix product $\bar{O}_m\bar{O}_{m-1}...\bar{O}_{l+1}$ need be considered.

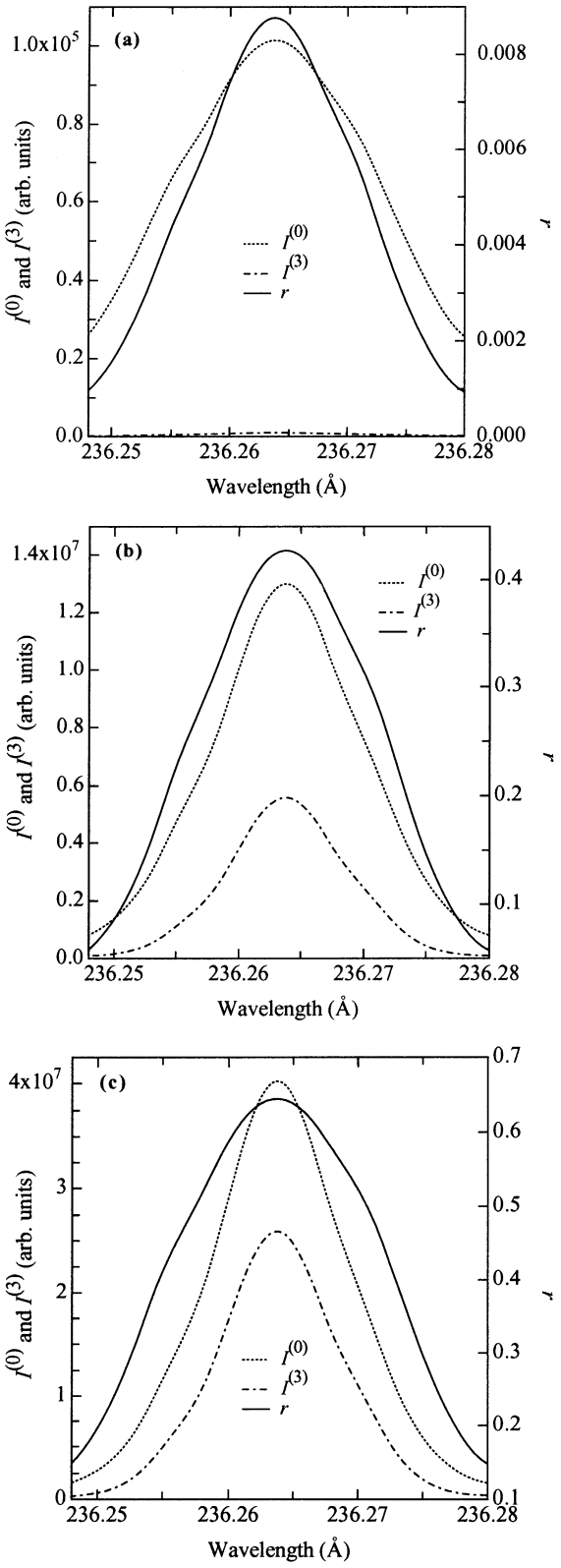

Fig. 2. Finite Stokes parameters $I^{(3)}$ and $I^{(0)}$, and $r = I^{(3)}/I^{(0)}$ for the Ge^{22+} 2−1 lasing line (23.6 nm), as a function of wavelength. Injector length is 0.5 cm. Amplifier lengths are (a): 1 cm, (b): 2 cm, (c): 3 cm. Density and temperatures, as in Figure 1.

The contribution $\sum_{l=1}^{m-1} \bar{O}_m \bar{O}_{m-1} ... \bar{O}_{l+1} \mathbf{V}_l$ to the Stokes vector then reduces to the 2-components vector $\mathbf{I}_1$:

$$\mathbf{I}_1 = \sum_{l=1}^{m-1} \begin{pmatrix} \cosh\left[\sum_{i=l+1}^{m} \Lambda_{1i}(z_i - z_{i-1})\right] & \sin\left[\sum_{i=l+1}^{m} \Lambda_{1i}(z_i - z_{i-1})\right] \\ \sinh\left[\sum_{i=l+1}^{m} \Lambda_{1i}(z_i - z_{i-1})\right] & \cosh\left[\sum_{i=l+1}^{m} \Lambda_{1i}(z_i - z_{i-1})\right] \end{pmatrix} \times \begin{pmatrix} V_l^{(0)} \\ V_l^{(3)} \end{pmatrix} \exp\left[\sum_{i=l+1}^{m} G_i^{(0)}(z_i - z_{i-1})\right]. \quad (14)$$

For a circularly polarized incident beam $\mathbf{I}_0[\equiv \mathbf{I}(z_0)]$ is such that $I_0^{(1)} = I_0^{(2)} = 0$. The contribution arising from the incident beam, namely $\bar{O}_m \bar{O}_{m-1} ... \bar{O}_2 \bar{O}_1 \mathbf{I}(z_0)$, is then replaced by the 2-components vector $\mathbf{I}_2$:

$$\mathbf{I}_2 = \begin{pmatrix} \cosh\left[\sum_{i=1}^{m} \Lambda_{1i}(z_i - z_{i-1})\right] & \sinh\left[\sum_{i=1}^{m} \Lambda_{1i}(z_i - z_{i-1})\right] \\ \sinh\left[\sum_{i=1}^{m} \Lambda_{1i}(z_i - z_{i-1})\right] & \cosh\left[\sum_{i=1}^{m} \Lambda_{1i}(z_i - z_{i-1})\right] \end{pmatrix} \times \begin{pmatrix} I_0^{(0)} \\ I_0^{(3)} \end{pmatrix} \exp\left[\sum_{i=1}^{m} G_i^{(0)}(z_i - z_{i-1})\right]. \quad (15)$$

The populations of the laser states (see Fig. 1) have an effect on the radiative-transfer problem, through the components given by equations (3-7). In other words, the intensity of the X-ray beam, which in the saturation regime determines the populations (rate equations, Ref. [16]), modifies the polarization state of the outgoing beam. The non-zero Stokes parameters $I^{(0)}$ and $I^{(3)}$ are given by equations (13-15). Let us represent $I^{(0)}$, $I^{(3)}$, and $I^{(3)}/I^{(0)}$, for the Ge^{22+} 2−1 line, when a σ_+ wave is seeded in the amplifier. In Figure 2 the injector length ($l_{\rm inj}$) is 0.5 cm and the amplifier length ($l_{\rm amp}$) varies. A large degradation of the initial polarization state occurs over the entire spectrum of the output, for the smaller $l_{\rm amp}$. The difference between $I^{(0)}$ and $I^{(3)}$ decreases for increasing $l_{\rm amp}$ showing that the radiation tends to recover the initial right-circular polarization. In Figure 3, $l_{\rm amp} = 1$ cm and we vary the injector length. The same features as above, but more pronounced, are observed. It is clear from the ratio of the Stokes parameters that the degree of circular polarization is less attenuated in the line core than in the wings of the output.

We now define a vector $\mathbf{D}$ whose r components ($r = 1-3$) are polarization rates:

$$D^{(r)} = I^{(r)}/I^{(0)}, \quad (16)$$

where the four Stokes parameters are integrated over frequency. We have $-1 \leq D^{(r)} \leq 1$. In our case $D^{(1)} = D^{(2)} = 0$, *i.e.*, the output cannot be linearly polarized. $D^{(3)}$ is the difference between the relative intensity of right-circular polarization, and that of left-circular polarization. Table 1 shows $D^{(3)}$ for the

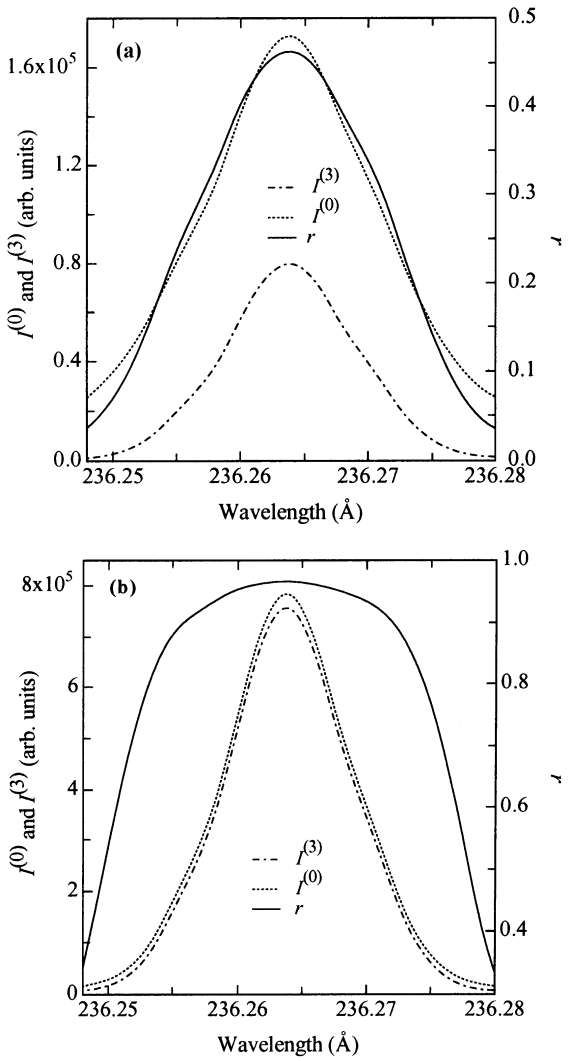

Fig. 3. Same as Figure 2. The amplifier length is 1 cm. Injector lengths are: (a): 1 cm, (b): 1.5 cm.

Table 1. Rate of circular polarization of the Ne-like Ge 2−1 line (23.6 nm), for various injector and amplifier lengths (cm). Density and temperatures, as in Figure 1.

amplifier→ injector↓	1	1.5	2	2.5	3
0.5	0.005	0.0813	0.328	0.463	0.546
1	0.302	0.716	0.828	0.868	0.891
1.5	0.918	0.956	0.969	0.975	0.978

Ne-like Ge 2−1 line. As clearly seen, the rate of circular polarization varies by a large amount when $l_{\rm inj}$ and $l_{\rm amp}$ vary, but it does not suffer an important degradation if the intensity of the incident beam is large ($l_{\rm inj} \geq 1.5$ cm) and the amplifier length is important. $D^{(3)}$ decreases from its initial value, namely 1, for the smallest amplifier lengths, due to an amplification of the σ_- wave. As σ_+ -seeded wave- is amplified more efficiently than σ_-, $D^{(3)}$ increases rapidly above a sufficiently large length.The incident-beam intensity $[I_0^{(0)}]$ plays the leading role in the final polarization state. It is also responsible for population migrations in each laser level, yielding a finite atomic orientation, thus enhancing the contribution of the medium to the final polarization state. However, this effect is attenuated by the electron-ion collisions which tend to equally re-distribute the ions between the states of each level (see Ref. [16]). The ion-ion collisions are much less efficient, in particular because the ion density is about twenty times smaller than the electron density.

To conclude, the solution of the RTE is obtained from a rigorous and new approach which is useful for the knowledge of the polarization evolution in soft-X-ray lasers, and which can be extended without major difficulty to other fields such as astrophysics and ICF plasmas. In order to assess the validity of our approach and to evaluate the role of elastic collisions on the output polarization, we plan an experiment at the LULI laser facility (École Polytechnique), in a configuration of injector-amplifier. Multilayers mirrors will be used to polarize the injector -unpolarized-output providing a circularly polarized beam at the entry of the amplifier.

References

1. D.L. Matthews *et al.*, Phys. Rev. Lett. **54,** 110 (1985).
2. *X-Ray Lasers 1996, Proceedings of the Fifth International Colloquium on X-ray lasers*, edited by S. Svanberg and C.-G. Wahlström, IOP Conf. Ser. **151** (Institute of Physics, Bristol, 1996).
3. B. Rus *et al.*, Phys. Rev. A **55,** 3858 (1997).
4. D.M. O'Neill *et al.*, Opt. Commun. **75,** 406 (1990).
5. S. Wang *et al.*, J. Opt. Soc. Am. B **9,** 360 (1992).
6. J. Zhang *et al.*, Phys. Rev. Lett. **78,** 3856 (1997).
7. J.E. Trebes *et al.*, Phys. Rev. Lett. **68,** 588 (1992).
8. R.L. London *et al.*, Phys. Rev. Lett. **65,** 563 (1990).
9. B. Rus *et al.*, Phys. Rev. A **51,** 2316 (1995).
10. T. Kawachi *et al.*, Phys. Rev. Lett. **75,** 3826 (1995).
11. C.H. Skinner *et al.*, J. Microsc. **159,** 51 (1990).
12. R.A. London *et al.*, Appl. Opt. **28,** 3397 (1989).
13. F. Albert *et al.*, Opt. Comm. **142,** 184 (1997).
14. L.B. Da Silva *et al.*, Phys. Rev. Lett. **74,** 3991 (1995).
15. D. Benredjem *et al.*, Phys. Rev. A **56,** 5152 (1997).
16. D. Benredjem *et al.*, Phys. Rev. A **55,** 4576 (1997).
17. B. Talin *et al.*, Phys. Rev. A **51,** 1918 (1995).
18. E. Landi Degl'Innocenti, Sol. Phys. **85,** 3 (1983).
19. *Numerical Radiative Transfer*, edited by W. Kalkofen (Cambridge University Press, UK, 1987).